



NUMERICAL AND EXPERIMENTAL INVESTIGATION OF A PULVERIZED COAL MILL DUCT SYSTEM IN THE SOMA B THERMAL POWER PLANT BY PLANT PERFORMANCE TESTS

Ali Bahadır OLCAY*, Murat KAHRAMAN** and Selçuk ATAŞ***

*Yeditepe University, Mechanical Engineering Department, Atasehir, Istanbul, Turkey
bahadir.olcay@yeditepe.edu.tr

**Energy Institute, TUBITAK Marmara Research Center, 41470 Gebze, Kocaeli, Turkey
murat.kahraman@tubitak.gov.tr

***Energy Institute, TUBITAK Marmara Research Center, 41470 Gebze, Kocaeli, Turkey
selcuk.atas@tubitak.gov.tr

(Geliş Tarihi: 07.03.2016, Kabul Tarihi: 16.06.2016)

Abstract: In a pulverized coal-fired (PCF) thermal power plant (TPP), mixture of coal, air and gas is supplied into the furnace volume via the mill duct system and coal/air distribution should ideally be maintained as homogeneous as possible to ensure an efficient combustion. The phenomenon of coal/air flow in the mill duct system has been so far an important issue in terms of boiler efficiency while this process has not been deeply understood yet. In this study, the flow of coal/air/gas mixtures in the mill duct system of Soma B TPP boiler was investigated to evaluate the performance of the boiler and it was found that boiler efficiency was directly affected by the high unburned carbon ratio especially with particle sizes larger than 500 μm in the bottom ash particles. Coal/air flow in the mill duct system in the Soma B TPP was numerically modeled to characterize the flow behavior of the coal particles and gas mixture. The model was validated with plant real time operation data obtained from field measurements. Particle distribution between the lower level burner ducts was found to be non-homogenous particularly sizes larger than 230 μm based on the simulation results. The main reasons behind the non-homogenous coal/air distribution were studied according to the validated model and two new mill duct system design alternatives (ND-01 and ND-02) were designed to resolve these issues. Base case and alternative design simulation results were compared with each other and it was realized that more homogenous particle disturbance was obtained in the mill duct system especially for the particle sizes larger than 230 μm in ND-01 design.

Keywords: pulverized coal, duct flow, coal-fired thermal power plants, CFD

SOMA TERMİK SANTRALİNDE KÖMÜR DEĞİRMEN KANAL SİSTEMİNİN SANTRAL PERFORMANS TESTLERİ YARDIMIYLA NÜMERİK VE DENEYSEL OLARAK İNCELENMESİ

Özet: Pülverize kömür yakan bir termik santralde kömür, hava ve gaz karışımı ocak bölgesine değirmen kanal sistemi ile beslenir. Verimli bir yanma için kömür/hava dağılımının ideale yakın derecede homojen olarak sağlanması gerekmektedir. Değirmen kanal sisteminde kömür/hava akışı olayı kazan verimliliği açısından oldukça önemli bir konu olup bu proses hala derinlemesine anlaşılamamış durumdadır. Bu çalışmada, kazan performansını değerlendirmek amacıyla Soma B Termik Santralinin değirmen kanal sistemindeki kömür/hava/gaz karışımlarına ait akış incelenmiş olup kazan veriminin özellikle taban külü partikülleri bünyesindeki 500 μm üstü yanmamış karbon miktarından direkt olarak etkilendiği görülmüştür. Soma B Termik Santralinde değirmen kanal sistemindeki kömür/hava akışı kömür partikülleri ve gaz karışımının akış davranışını karakterize etmek üzere nümerik olarak modellenmiştir. Model saha ölçümleri ile elde edilen gerçek zamanlı santral işletme verileri ile doğrulanmıştır. Simülasyon sonuçlarına göre 230 μm üstü partiküllerin alt seviye yakıcı kanalları arasındaki dağılımının homojen olmadığı görülmüştür. Doğrulanmış model baz alınarak homojen olmayan kömür/hava dağılımının temel sebepleri araştırılmış ve bu sorunları çözmek için iki adet yeni değirmen kanal sistem alternatifi (ND-01 ve ND-02) tasarlanmıştır. Mevcut durum ve alternatif tasarımlara ait simülasyon sonuçları karşılaştırılmış ve özellikle 230 μm üzeri partiküller için ND-01 tasarımı ile değirmen kanal sisteminde daha homojen bir partikül dağılımı elde edildiği görülmüştür.

Anahtar Kelimeler: pülverize kömür, kanal akışı, kömür yakıtlı termik santraller, HAD

NOMENCLATURE

η_B	Total boiler efficiency [%]
L_i	Individual losses in boiler [%]
v_p	Velocity of particle [m/s]
t	Time [s]
F_A	Drag force [N]
v_g	Gas velocity [m/s]
v_p	Particle velocity [m/s]
g	The gravitational acceleration [m/s ²]
μ	The gas viscosity [N·s/m ²]
ρ_p	The density of the particle [kg/m ³]
d_p	The diameter of the particle [m]
C_D	The drag coefficient of the particle [-]
Re	Reynolds number
x_p	Location of the particle [m]
m_p	Particle mass [kg]
R	Universal gas constant [J mol ⁻¹ K ⁻¹]
T	Temperature [K]
X_{O_2}	Mass fraction of O ₂ [-]
M_{O_2}	Molecular weight of O ₂ [-]
R_T	Overall reaction rate [g cm ⁻² s ⁻¹ atm ⁻¹]

Abbreviations

PCF	Pulverized coal-fired
TPP	Thermal power plant
CFD	Computational Fluid Dynamics
ESP	Electrostatic Precipitator
ASTM	American Society for Testing and Materials
DPM	Discrete Phase Model
RANS	Reynolds Average Navier-Stokes
RSM	Reynolds Stress Model
ASME	The American Society of Mechanical Engineers
PTC	Performance Test Codes

INTRODUCTION

In pulverized coal-fired (PCF) thermal power plants (TPPs), coal burners are typically used to inject pulverized coal to the boiler furnace combustion zone. After coals are pulverized and classified to the desired sizes in the mill, they are generally transferred to the coal burners with the guidance of primary air and flue gas mixtures. Besides, the flow rate of coal and air should be homogeneously balanced for each duct of the mill to obtain efficient coal combustion (Chen et al., 1992; Kitto and Stultz, 2005). Each mill in a TPP has its own independent mill duct configuration; therefore, both balancing and tuning of coal/air mixture should be performed for each individual mill. This phenomenon plays a key role for combustion performance and emission control in TPPs. Furthermore, the acceptable level of unburned carbon in fly and bottom ash in the boiler can be obtained by providing coal/air balance in the mill ducts for each burner. Both the slagging and fouling in the boiler can be reduced by keeping the furnace exit temperature within the design limits of the coal softening temperature based on properties of the coals (Kitto and Stultz, 2005). As a result, a balanced

coal/air flow in the mill duct system can prevent water-wall wastage and tube over-heating. On the other hand, unbalanced coal/air flow into the burners can cause non-homogeneous combustion inside the furnace yielding increase in loss of ignition with a decrease in efficiency of the TPP (Storm Technologies, 2004).

The importance of pulverized coal flow in a mill duct system was earlier studied by Huber and Sommerfeld (1994). They examined the development of particle concentration distribution in dilute phase pneumatic conveying in a pilot-scale test facility consisting of different pipe configurations. They reported that wall roughness was an effective parameter of the flow characteristics. They also stated that increasing bend radius provided more uniform particle distribution in the pipe. A numerical study for the mill duct system of a thermal power plant was performed by Kozic et al. (2010). They determined the critical locations exposed the most intense wear in the mill duct system based on the numerical results. Dodds et al. (2011) numerically investigated the flow of coal/air mixture in a mill-duct system for a PCF TPP. They discovered that computational fluid dynamics (CFD) results correlated with the operational data. They also observed that while the lower and upper mill-ducts biased coal flow with a more homogeneous coal distribution along the duct, the intermediate mill-duct had significant lower coal loading. Vijiapurapu et al. (2006) studied to balance coal/air mixture using CFD analysis. They pointed out that balanced clean air flow in the mill ducts does not result in a balance for coal flows through each burner. Orifices were sized according to coal/air pressure drop results obtained by CFD analyses to meet coal/air balance for the burners. The effects of the classifier vane settings on the pulverizer performance were investigated by Shah et al. (2009). They stated that a balanced distribution of coal in the mill ducts was an important phenomenon to sustain efficient combustion in PCF boilers. CFD simulations of coal/air flow in the mill ducts of an operating thermal power plant were performed in another study and the results of the experimental data were compared with numerical findings (Ferrin and Saavedra, 2013). Parham and Easson (2003) performed flow visualization and velocity measurements to compare the aerodynamic characteristics of a vertical spindle coal mill static classifier model. There are also studies focusing on dilute particulate flow through curved ducts. For example, Young et al. (2006) was being one of them detected significant gas-solid separation close to the outer wall of the curved duct with a slip velocity between gas and solid phase. The gas and solid velocities were similar to each other at the inner wall. In another study, three different multiphase flow models (Euler-Euler, Euler-Lagrange and E-L with modification) were used for modeling of an air/coal mixture flow through the pipeline with the built-in elbow and the results were compared (Wydrych et al., 2014). Atas et al. (2014) examined the performance of a PCF TPP mill separator numerically with the help of isokinetic sampling measurements. In addition, an increase in the separation efficiency was aimed by

designing alternative coal mill separators. Additional plates were used to control the coal particle flow in the mill classifier system; therefore, an increase in the separation efficiency of the mill was obtained. Blondeau et al. (2016) presented a new insight into the coal particle size distribution and coal flow distribution between burners in 660 MWe coal-fired power plant. They monitored online the particle size variation and the flow rate distribution to the burners by using a laser probe and microwave sensors. They also investigated the influence of varying the classifier speed on the coal particle size and flow distribution.

Both experimental and numerical studies of coal/air mixture's flow characteristics in the mill ducts typically provide significant information about the performance of TPPs. However, difficulty in balancing coal/air mixture in these ducts, long duration field-tests in very difficult conditions and stability of the operating conditions make this kind of study very challenging. The objective of this study is to evaluate the current status of the mill duct system of the Soma B TPP and investigate the causes of the non-homogenous flow in the system and finally provide recommendations for a more uniform coal/air mixture in the system. In this present study, the plant base case test results in the mill

ducts of the Soma B TPP were presented in terms of coal balancing and boiler efficiency. The numerical analysis of unknown dilute coal/air flow in the mill ducts of the Soma B TPP was investigated and verified based on the test results in the mill ducts to follow design modifications with modeling assumptions. Later, two alternative constructions were offered according to the output of the numerical analyses so as to obtain more homogenous coal particle distribution through coal burners.

METHOD

Plant performance tests

The Soma B TPP contains six units, each with an electrical capacity of 165 MWe. The TPP boilers is single pass with natural circulation, drum type boiler firing lignite and placed with six high-speed impact mills. Each unit utilizes a lignite-fired boiler with six horizontal air-swept mills with beaters. A classifier which is placed at the exit of the mill separates coarse particles and redirects them for further pulverization to the mill and transports fine particles to the burner. The specifications of the mill are shown in Table 1.

Table 1. TPP pulverizer properties

Pulverizer type	Horizontal air swept with beater and fan	
Number of pulverizers	6 total (5 main + 1 spare)	
Maximum coal capacity	37	[ton h ⁻¹]
Coal pulverization rate less than 1.000 μm	97-98	[%]
Coal pulverization rate less than 90 μm	50	[%]
Coal gas temperature after pulverizer	140	[°C]
Coal gas operation temperature after pulverizer	100 -180	[°C]
Pulverizer outlet trip temperature	≥ 220	[°C]
Pulverizer operation speed	450-650	[rpm]
Gas volumetric flow rate	25	[m ³ s ⁻¹]
Maximum pulverizer fan speed	90	[m s ⁻¹]
Extracted drying gas temperature for coal	925	[°C]

The operation of the mill duct system as shown in Figure 1 was analyzed in this study and description of the system is provided in the following steps (the numbering in the following steps can be seen in Figure 1). (1) The coal enters the pulverizer with 925°C gas withdrawn from the boiler. (2) The beater hammers break the coal to smaller pieces, and the coal drying process begins. (3) Broken and partially pulverized coal passes through the fan and the coal particles collide with the surfaces of the stator and rotor of the fan blades. During this process, the coal particles become smaller due to attrition and collision forces. (4) The pulverized coal particles move into the classifier volume. The gas and coal particle mixture exits from the pulverizer at a velocity of approximately 30-35 m/s from the classifier volume. (5) This high speed forces the coal particles passing to the radial region of the classifier. (6) However, all of the particles do not follow this process.

The coarse particles collide first with the radial surface of the classifier and lose some of their kinetic energy. If the coarse particles lose enough energy due to the collision, then the large and heavy coal particles move downward and turn back towards the mill for further pulverization from the return outlet of the pulverizer. (7) On the other hand, the small and fine coal particles at 100-180°C follow the flow stream to the mill ducts without colliding with the classifier surface because they are small enough to follow the flow stream. After the classifier, these fine coal particles travel pneumatically in the mill duct system up to the level of 10 meters and they are divided for lower and upper burners (8, 9) at 13 meters and (10, 11) at 17 meters. Another separation occurs for upper and lower burners at these levels. In other words, pulverizers in the Soma B TPP have four fuel conduits (8, 9, 10, 11) supplying the fuel to the combustion chamber.

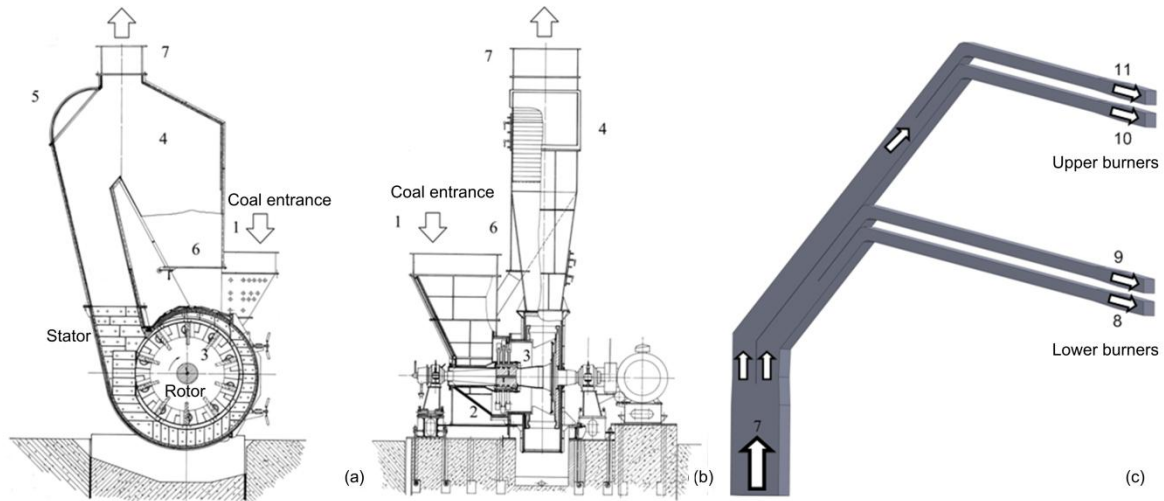


Figure 1. The front (a), the cross sectional view (b) of the mill and the duct system geometry between the mill and the furnace entrance (c).

In the TPP tests, ash samples from the boiler bottom ash extractor and electrostatic precipitator (ESP) hoppers were received to analyze unburned carbon rates in their contents. The amounts of unburned carbon in these samples were acquired by the ultimate analyses with a standard of ASTM D-5357. Gravimetric tests were conducted at the boiler to determine the ash proportion between bottom and fly ash by measuring the quantity of the bottom ash for fifteen minutes along with determining total ash of burning coal at the same time. The fly ash temperature was assumed to be the same as flue gas temperature at the exit of the air heater. Bottom ash temperatures were determined by an infrared thermometer (Fluke 66 - with laser-guided sighting) during measurements. Ultimate/proximate analyses were carried out for coal samples to evaluate the properties of burning coal. LUCO Truspec instrument for carbon, hydrogen and nitrogen with a standard of ASTM D-5357 was utilized in the ultimate analyses. Sulphur content was also determined by the same instrument with a standard of ASTM D-4239. Total boiler efficiency (η_B) in terms of coal gross heating value can be calculated from the equation below by individual losses in the boiler as illustrated in Figure 2.

$$\eta_B(\%) = 1 - \sum_{i=1}^{10} L_i \quad (1)$$

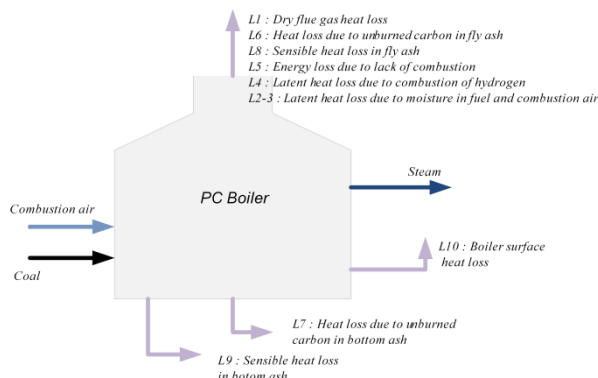


Figure 2. Energy inputs-outputs and losses at the boiler

During the TPP operational tests, the coal samples from the coal mill ducts were collected by using a sampling method at isokinetic conditions. The total pressure, static pressure, and gas temperature were measured to specify isokinetic conditions in Duct A, B and C as shown in Figure 3. The coal samples were obtained at these measurement points by a separation of coal and gas in a cyclone. There were 13 particle sample locations along one measurement port and the sampling time for each port was 10 seconds. The classification of the coal samples were carried out by sieving them in a vibratory sieving machine with vibration amplitude of 85 at 15 minutes.

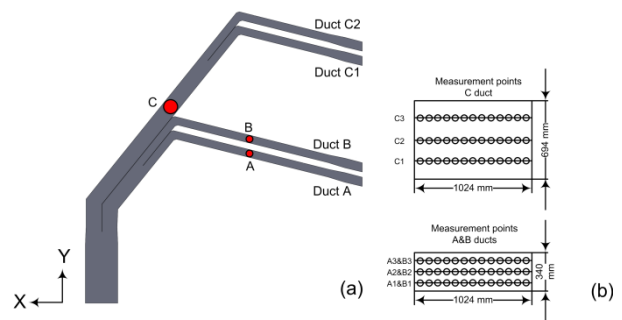


Figure 3. Coal-air ducts (a) and cross section view of measurement points (b)

Numerical analysis

In the mill duct system, a pulverized coal particle follows the path of the flow stream when the gravitational force acting on the particle is not larger than the drag force due to gas flow. If the amount of coal particles in the gas volume is less than 10%, this flow is typically considered to be a dilute mixture. In addition, it was assumed that particle-to-particle interaction and collisions did not occur for dilute gas-particle flows. In this study, flow characteristics was predicted by the commercial software FLUENT. In the analyses, while the Reynolds-Averaged Navier-Stokes (RANS) and continuity equations were solved for gas

fluid flow, the particle flow was computed by use of a discrete-phase model (DPM). A DPM was valid because the solid-volume ratio stayed less than 10% in this analysis (Dodds et al., 2007). In the numerical control volume, velocities of particles (v_p) were obtained by the equation:

$$\frac{dv_p}{dt} = F_A(v_g - v_p) + g \quad (2)$$

where g was the gravitational acceleration, t was the time and the initial velocities of the particles were assumed to be equal to the gas velocity (v_g).

$$v_p(0) = v_g(0) \quad (3)$$

$F_A(v_g - v_p)$ was the drag force exerted on the unit mass.

$$F_A = \frac{3}{4} \frac{\mu}{\rho_p d_p^2} C_D Re \quad (4)$$

where d_p , ρ_p and C_D were the diameter, the density and the drag coefficient of the coal particle respectively and μ was the gas viscosity. The fluid was assumed to be viscous and incompressible and Reynolds number (Re) was defined relative to the particle. Locations of coal particles (x_p) in the numerical control volume were obtained by Eq. (5).

$$\frac{dx_p}{dt} = v_p \quad (5)$$

The Reynolds number of the gas-phase flow was defined based on a hydraulic diameter of the duct by considering the duct cross-section dimension. The gas-phase flow velocity in the mill ducts was very high after the mill and the flow was in turbulent regime because Reynolds number at the inlet of the duct system was nearly 9×10^5 . Turbulent flow in the duct system was solved using Reynolds Stress Model (RSM) in steady state conditions. According to the literature survey (Atas et al., 2014; Kuan et al., 2007; Kuan et al., 2003), it was stated that accurate results could be achieved by using of RSM model. Moreover, an enhanced wall treatment approach was used for near-wall treatment in modeling turbulent flow to have a flexible mesh structure in the computational domain. Grid spacing along the flow spanwise direction was near enough to the wall to obtain adequate y^+ value (i.e., $y^+ \approx 1$) adjacent to the walls. Boundary conditions of the numerical solution were based on the operating conditions of the plant obtained during the measurements in the TPP. The coal flow rate was measured separately for each mill duct. The gas velocity at the inlet of the duct system was determined based on the measured total coal flow rate in the mill duct system. Nine different injection sizes were used to define particle size distributions at the inlet for the solid phase modeling according to the data obtained from the plant tests as shown in Table 2. The average

velocity profile was used at the inlet of the computational control volume because the distance from the mill outlet and the first elbow was long enough to satisfy the fully developed flow conditions inside the duct. Outlet of the mill ducts had an opening to the boiler furnace volume and the pressure inside the furnace was nearly at atmospheric conditions. Therefore, atmospheric pressure was assumed at the outlet of the mill ducts through the CFD analysis. Gas temperature was set to be 161°C as an inlet boundary condition in the mill duct system during the measurements and fluid was defined as air in that temperature in numerical analysis. All the required data were taken at steady-state conditions according to the TPP loads and only 2% load change was permitted during data acquisition.

Table 2. Coal particle diameter and flow rate for inlet boundary condition

Coal particle diameter (μm)	Flow rate (kg/s)
1,310	0.11
985	0.93
675	0.12
410	0.93
230	2.26
120	1.06
95	0.27
80	0.55
45	3.86
Total	10.09

The computational domain of the mill duct system was modeled by using a structured grid as illustrated in Figure 4.

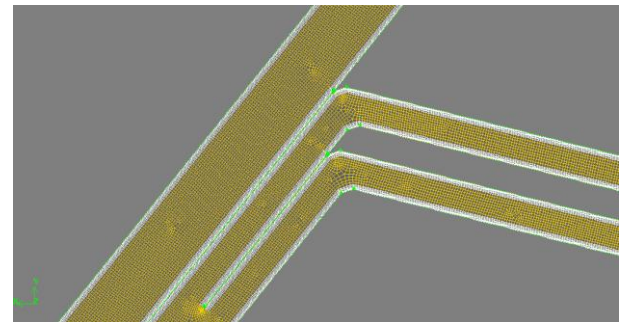


Figure 4. Detailed view of the grid mesh structure

The orthogonal mesh quality ranges from 0 to 1 where values close to the 0 corresponds to low quality. In the present study, the minimum orthogonal value was 0.89 implying the presence of high quality mesh in the computational domain. According to the definition of skewness, while a value of 0 indicates the best cell, a value of 1 represents a completely degenerate cell. In the current study, the average and maximum skewness values were obtained as 0.03 and 0.5, respectively implying the presence of the high quality elements in the computational domain.

Table 3. Numerical analyses parameters

Gas density	0.813	[kg m ⁻³]
Gas temperature	161	[°C]
Inlet velocity	22.3	[m s ⁻¹]
Outlet pressure – gage	0	[Pa]
Particle density	1,000	[kg m ⁻³]
Restitution coefficient (normal)	0.5	-
Restitution coefficient (tangent)	0.9	-

Grid independency tests were performed based on pressure coefficient along the geometry by changing the mesh size and the number of elements in the domain. Total of 1,739,630 hexahedral cells were assigned in the model and number of cells was high enough for an independent solution when the variation of the pressure coefficient along the duct system was remained below 0.6%. Some of the numerical analyses parameters were given in Table 3.

RESULTS AND DISCUSSION

Table 4. Results of the first law energy analysis of PC boiler

Losses (%)		Case 1	Case 2	Case 3	Case 4	Average	Absolute Uncertainty	Design Values
L ₁	Heat loss due to dry flue gas	7.2	7.2	7.9	6.9	7.3	0.26	7.8
L ₂	Latent heat loss due to moisture in fuel	4.1	4.5	4.7	4.4	4.4	0.15	4.6
L ₃	Latent heat loss due to moisture in combustion air	0.06	0.05	0.04	0.04	0.05	0.01	0.23
L ₄	Latent heat loss due to combustion of hydrogen	2.1	2.6	2.4	4.0	2.8	0.25	2.6
L ₅	Energy loss due to CO in flue gas	0.2	0.2	0.1	0.1	0.1	0.03	0.3
L ₆	Energy loss due to unburned carbon in fly ash	1.6	2.0	1.6	1.4	1.6	0.15	0.4
L ₇	Energy loss due to unburned carbon in bottom ash	5.7	6.5	4.3	5.0	5.3	0.36	0.8
L ₈	Heat loss due to sensible heat in fly ash	0.4	0.4	0.5	0.5	0.5	0.03	0.4
L ₉	Heat loss due to sensible heat in bottom ash	1.2	1.3	1.3	1.3	1.3	0.10	1.3
L ₁₀	Heat loss from boiler wall heat transfers	1.8	1.9	1.8	1.7	1.8	0.11	0.5
Total loss in the boiler		24.3	26.6	24.7	25.2	25.2	1.45	18.9
Total efficiency in the boiler		75.7	73.4	75.3	74.8	74.8	1.45	81.1

It was obtained from the energy analyses that the main energy losses were unburned carbon losses (L6, L7) both for fly and bottom ash and loss from the boiler wall heat transfers (L10). As L10 was related to heat insulation of the boiler, mainly operation related losses L6 and L7 were investigated in this study. According to measurements, the unburned carbon loss ratio was calculated as averagely 1.6% and 5.3% for energy loss ratio due to unburned carbon in fly ash (L6) and in bottom ash (L7), respectively. As compared with design values, approximately 4-7 times more degradation was observed for these losses. These high value losses could be mainly due to two main reasons: one being because of the low content of oxygen supplied the boiler or the other being due to the poor pulverization of the coal. Conversely, it was observed that the lack of oxygen

Plant test results and evaluation of boiler efficiency

The energy analysis by calculating individual losses were performed in the boiler control volume for four cases: boiler loads being at the rates of 82%, 84%, 85% and 91%. According to the used indirect loss method, average total PCF boiler efficiency was found to be 74.8% with ±1.45% absolute uncertainty at a confidence level of 95% with respect to Gross Calorific Value (GCV). The uncertainty analyses were performed with a method described in ASME PTC 19.1.1998, Test Uncertainty. As the design value for this PCF boiler was appointed 81.1%, a degree of degradation in the boiler performance was observed with a rate of 7.7% as provided in Table 4. These results indicates that the boiler must burn approximately 7.7% more coal to generate the same level of energy by producing more emissions (SO_x, NO_x, fly ash, dust) totally.

could not be a main reason for the unburned carbon loss based on the analyses from the dry flue gas losses. This was due to the fact that the excess air being high enough for full combustion and the low carbon monoxide ratios were recorded at the exit of the boiler.

On the other hand, in order to specify the main reason, the fly ash samples from the boiler was sieved to obtain both lower and higher sizes of ash particles than 74 µm. Later, the unburned carbon contents were examined in the sieved samples as shown in Figure 5(a). Average of 0.46% unburned carbon was observed in the ash particles lower than 74 µm from the analyses. This showed that if the coal was pulverized and classified better, then the unburned carbon loss in the fly ash would be decreased with reduced heat losses.

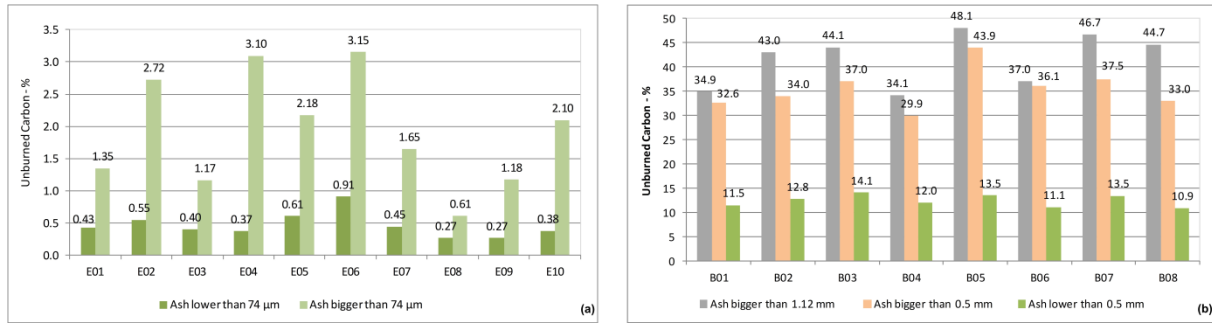


Figure 5. Unburned carbon ratios in (a) fly ash samples and in (b) bottom ash samples

Limits in operational experience indicated that 60-70% of pulverized coal passed through the sieve with a size of 74 μm and only 2% of them were retained on the sieve with a size of 297 μm. In pulverized coal combustion, the coal particles should be finely ground for rapid ignition. Coarse particles larger than 150 μm were the primary cause of unburned carbon loss. Thus, a minimal amount of coarse particles was desired to obtain maximum combustion efficiency. Thus, pulverization and classification have an important role

to provide desired particle size and increase reactivity of coal combustion (Kitto and Stultz, 2005; Singer, 1991). Additionally, bottom ash samples were also sieved and separated into two parts as smaller and larger size than 500 μm similar to the fly ash analyses. Then, their unburned carbon contents were examined as shown in Figure 5(b). It was observed that most of the unburned carbon (35-40%) was inside the ash above 500 μm and approximately 80% of total mass of the bottom ash remained above 500 μm.

Table 5. Results of coal sample sieve analysis for the measurements in the coal-air ducts

Sieve mesh size (μm)	A1	A2	A3	Aa*	B1	B2	B3	Ba*	C
	On the sieve (%)								
1120	4.56	1.39	0.36	1.74	0.92	0.25	0.05	0.25	1.14
850	4.35	1.74	0.47	1.85	1.34	0.33	0.15	0.39	1.06
500	15.61	8.53	2.53	7.76	7.16	3.15	1.26	2.82	4.89
315	15.99	13.12	6.53	11.06	11.85	8.89	5.41	7.66	7.94
140	23.47	27.29	24.25	25.06	23.68	26.69	25.71	25.80	20.66
100	7.72	10.24	13.46	10.97	9.83	11.83	15.03	13.06	10.45
90	1.84	2.49	3.98	2.96	2.53	3.04	4.14	3.49	2.93
71	3.78	4.95	6.71	5.40	5.46	5.67	8.44	6.95	6.06
Receiver	22.68	30.24	41.71	33.20	37.22	40.15	39.80	39.57	44.87

*Aa and Ba are average mass flow rate weighted values of coal sample sieve analysis A1, A2,A3 and B1, B2,B3 respectively.

As a result of these analyses, it was realized that the unburned carbon loss from the bottom of the boiler was the main reason for the efficiency loss of the boiler. The aim of better combustion was mainly to equalize the mass flow rate of coal particles to be lower than 150 μm for all of the mill ducts. Furthermore, it was desired to feed them to the mill ducts Duct B and Duct C1 for the coal particles larger than 150 μm so that they would have enough time for burning instead of falling down to the boiler hooper as unburned carbon. It was observed that most of the larger coal particles were fed from Duct A based on the TPP coal measurements in the current operation (Table 5). While 52.5% of total coal was measured below 140 μm particle size in Duct A, this rate was nearly 63.1% in Duct B. This implies that large coal sizes were transferred by the burner in Duct A in

the current operation of the TPP. Besides, this was the same for the coal sizes larger than 1 mm. While 1.7% of the coal amount larger than 1.12 mm was fed from the burner in Duct A, 0.2% of the total amount of this size was fed from the burner in Duct B. Furthermore, the burners were inclined down to the boiler with an angle of 12° as can be seen in Figure 3(a). This configuration allowed coal particles to naturally go down with its velocity at the burner exit.

Numerical analysis results

A numerical model was generated from the geometry of the mill duct system as shown in Figure 3 and the model was validated by real operating data measured in the Soma B TPP. In the first stage of the numerical analysis,

gas flow (Eulerian region) was converged by excluding the coal particles. Then, the numerical simulation results of the normalized gas velocities based on the inlet velocity (u_{in}) at the measurement points (shown in Figure 3(b)) were compared with the results obtained at plant measurements (Figure 6).

Results of numerical solution correlated well with the field measurements except for the measurement point B1 in Figure 6. Only $\pm 2\%$ load change was permitted, so this can be seen as the main reason for incompatibility of the velocity result at B1 point.

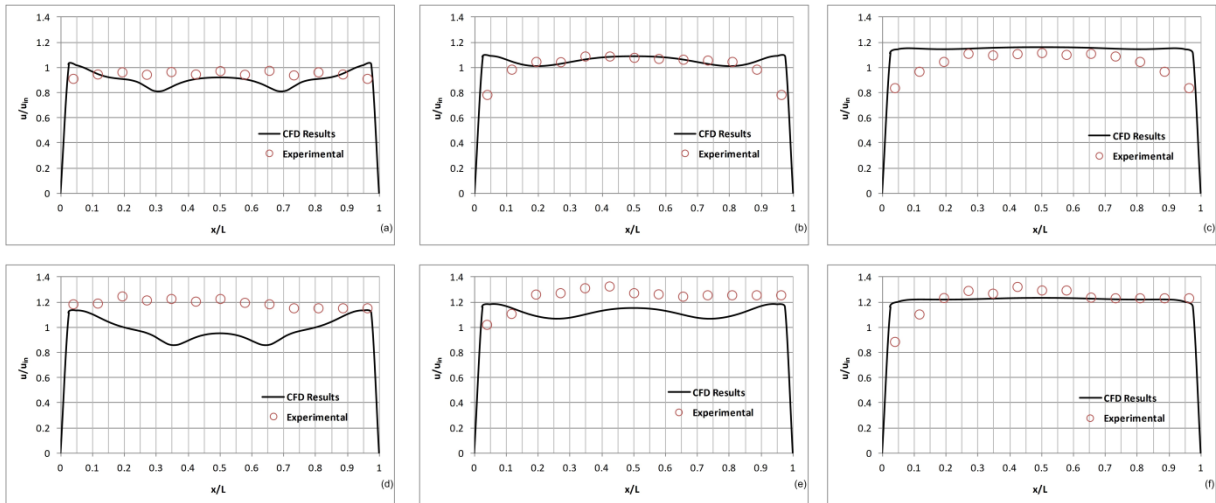


Figure 6. Base case velocity profiles (u/u_{in}) at the measurement points of (a) A1, (b) A2, (c) A3, (e) B1, (e) B2 and (f) B3

Once the CFD model was validated with the field measurements, solid-gas two-phase flow (Lagrangian region) simulations were performed. Some coal samples were taken from the coal duct system at isokinetic conditions in the TPP measurements and they were subjected to sieve analysis to obtain mass percentages according to their particle sizes as seen in Table 5. These distributions were utilized as an input value for the inlet boundary condition of the numerical analysis. Results of the numerical analysis were compared with the coal particle size distribution in Duct A, B and Duct C as shown in Figure 7 and the results were seen as quite consistent with the operation data of the TPP.

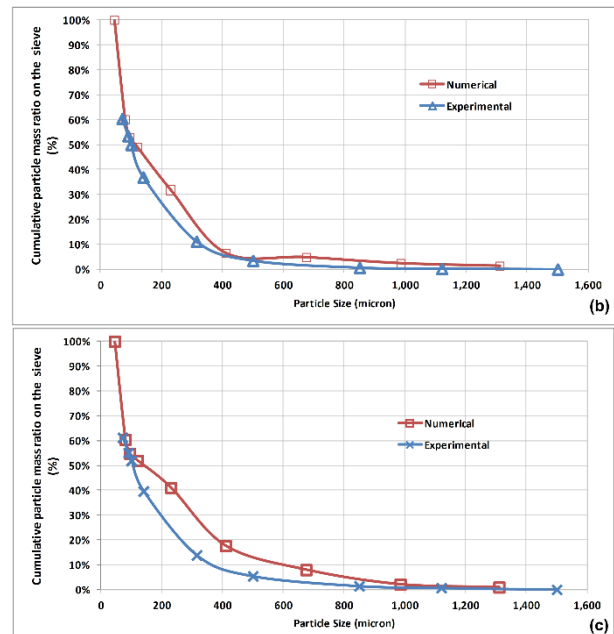


Figure 7. Coal particle size distribution (a) Duct A (b) Duct B (c) Duct C

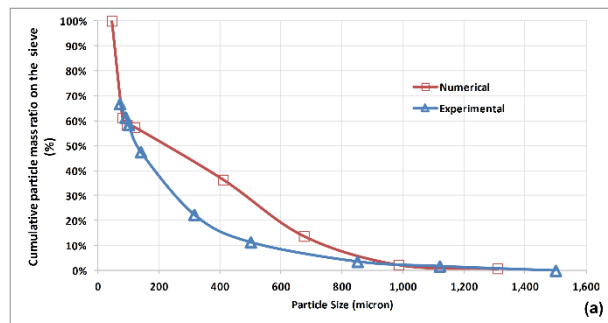


Figure 8 shows velocity profile in the mill duct system and trajectories of coal particles for 45, 120, 410 and 985 μm sizes obtained from CFD analysis. As it is seen from the figures, coal particles form as a rope while moving inside the duct and the coal in sizes 45 and 120 μm keep tracking of flow stream. However, larger coal particles were obtained to be not dominated by the flow but by the resultant forces from flow and coal inertia.

The following results were obtained after evaluating the numerical analysis results validated with TPP measurements (Table 6);

- While half of the total coal flow rate (51%) nearly flowed in Duct C, the other half (49%) nearly flowed in Duct A and Duct B based on the findings of the numerical analysis. These results were consistent with the field measurements.
- While 31.00% of the total coal flow rate flowed in Duct A, 19.03% of the total coal flow rate flowed in

Duct B. This result was also in agreement with the field measurements.

- Although 62% mass flow rate of the particles size between 45 and 230 μm was directed to Duct B and

Duct C2, 72% mass flow rate of the particles size between 410 and 1310 μm was directed to Duct A and Duct C1.

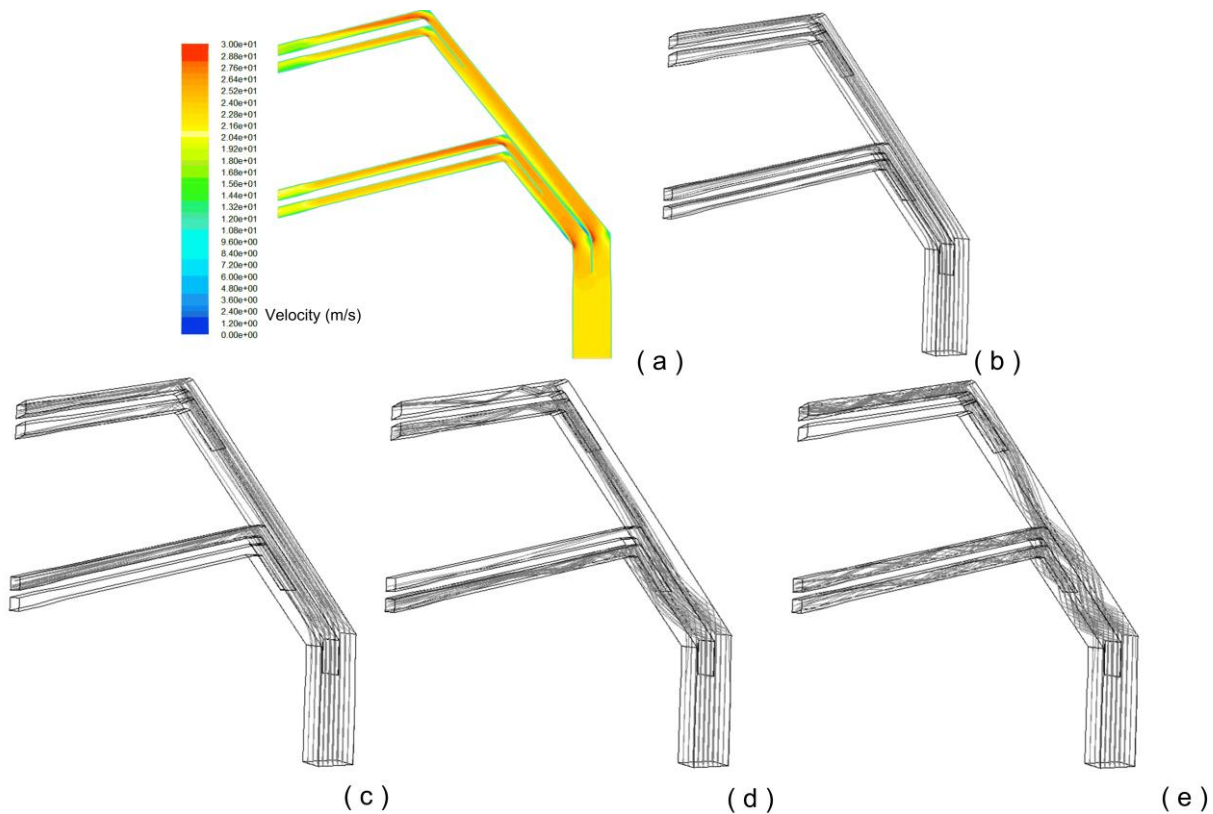


Figure 8. (a) Velocity (m/s) contours of duct system and tracks of coal particles for (b) 45, (c) 120, (d) 410 and (e) 985 μm sizes

Table 6. Coal mass flow distribution among duct system outputs (CFD results vs. TPP measurements)

		CFD results particle size (μm)										TPP measurements		
		45	80	95	120	230	410	675	985	1310	Total	Total > 500 μm	Total	Total > 500 μm
Duct A	Particle mass flow (kg/s)	0.71	0.05	0.02	0.01	0.38	0.42	0.21	0.03	0.02	1.84	0.26	2.26	0.26
Duct B		1.19	0.22	0.12	0.52	0.76	0.05	0.07	0.03	0.04	3.00	0.14	2.81	0.10
Duct C1		0.75	0.07	0.03	0.07	0.94	0.28	0.25	0.00	0.04	2.43	0.29	4.67	0.25
Duct C2		1.16	0.20	0.11	0.46	0.19	0.19	0.03	0.06	0.01	2.41	0.10		

Particle distribution in Duct A and Duct B outlets was not homogenous based on the results in Table 6 particularly for 230 μm and sizes larger than 230 μm . Maximum particle mass fraction deviation from average mass fraction of the mill duct system for particles in the size of 410 μm , 675 μm , 985 μm and 1310 μm was observed as 20%, 19%, 25% and 17%, respectively. This made completion of combustion of the coarse coal particles in the furnace difficult. As a result of these findings, some constructive measures could have been taken in the mill duct system.

Another reason for the high unburned carbon was non-uniform mixture of the coal and combustion air in the combustion chamber. Coal burners could not exactly mix the coal and air for 100% combustion so fuel-rich and fuel-lean areas were formed during the combustion. Especially, in the fuel rich areas the unburned carbon

contents could be increased due the lack of air. Therefore, it should be examined the mixture of the coal and combustion air in the combustion chamber as a future work as well.

New coal duct design for better performance

It was observed that the pulverized coal size larger than 0.5 mm caused unburned carbon loss and had a tendency track through Duct A and Duct C1. Therefore, this condition was considered in the numerical studies for the new duct design and the total amount of coal at this size were tried to be decreased to some extent. As it is seen from the Figure 8, coal particles formed a rope while moving inside the duct and the coal in smaller sizes than 0.5 mm followed the track of flow stream. However, the coals in larger sizes were obtained not to

be dominated by the flow but by the resultant forces from both flow and coal inertias. Thus, it was necessary to disrupt the rope mechanism before entering into the burner ducts. In the last few decades, new burner designs have been developed to ensure homogenization of the coal-air mixture. In most of the pulverized coal burners, the homogeneity of coal/air mixture inside the burner was ensured by a venturi. These type designs have been easy for maintaining homogeneity and could be seen very commonly in similar systems. Motivated by the design of a venturi, a new design was offered by constructing a venturi before the separation of Duct A and B to sustain homogeneity of coal particles larger than 0.5 mm in Duct A and B of the existing TPP. Two new design alternatives, namely ND-01 and ND-02, were produced for the coal duct system as shown in Figure 9. The venturi throat was designed with an angle of 15° and of 20° for ND-01 and ND-02, respectively. These two new designs were considered in the studies of two phase flow modelling.

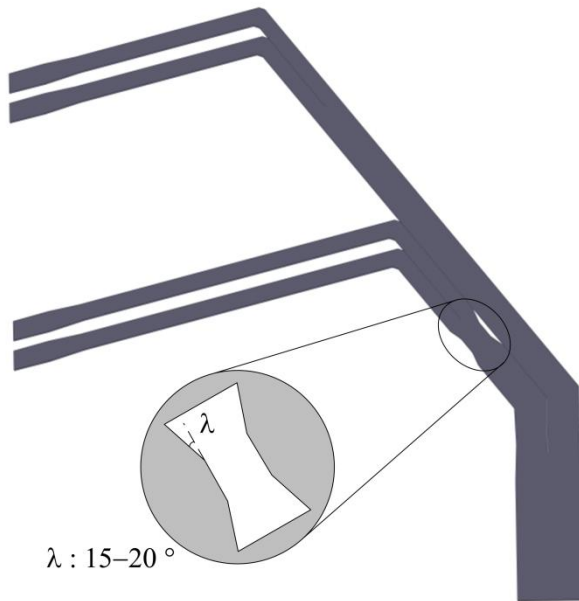


Figure 9. Schematic view of the alternative coal duct system design

Alternative duct system designs (ND-01 and ND-02) were not obtained with a significant effect on the disturbance in the duct system for the particle sizes in 45 μm, 80 μm, 95 μm and 120 μm. However, Figure 10 shows that the disturbance in the duct system for the particles in the size of 230 μm and in larger sizes than 230 μm were affected by the alternative duct system designs ND-01 and ND-02. As it was stated earlier, the main purpose of these alternative designs was to obtain more homogenous coal particle disturbance in Duct A and Duct B especially for the particles larger than 120 μm size. The homogeneity of the particle disturbance in ND-01 duct system was obtained to be more than ND-02 based on the results shown in Figure 10. For example, the maximum particle mass fraction deviation of Duct A and Duct B from the average mass fraction of the total duct system for 230 μm size particles was obtained to be

8.4%, 3.3%, and 8.0% for the base case, ND-01 and ND-02 simulations respectively.

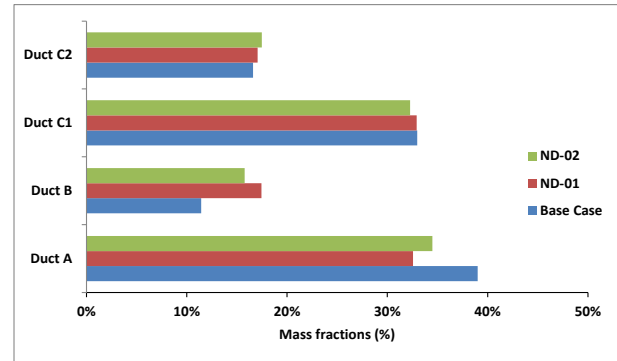


Figure 10. Coal distribution between duct outlets for 410 μm and bigger particle sizes

Generally, a coarse coal particle does not have enough time to complete its combustion and it is typically disposed from the boiler into the bottom ash or fly ash. One of the main reason for incomplete combustion of a coarse coal particle is due to extensive surface area of the coal particle. This phenomena was stated in the char combustion model of Baum and Street (1971).

$$\frac{dm_p}{dt} = -\pi D_p^2 \frac{\rho R T X_{O_2}}{M_{O_2}} R_T \quad (6)$$

where m_p is particle mass (g), t is time (s), D_p is diameter of particle (cm), ρ is density ($g\ cm^{-3}$), R is universal gas constant ($J\ mol^{-1}K^{-1}$), T is temperature (K), X_{O_2} is mass fraction of O_2 , M_{O_2} is molecular weight of O_2 and R_T was overall reaction rate ($g\ cm^{-2}\ s^{-1}\ atm^{-1}$). Particle diameter or particle surface area were one of the most important parameters affecting the combustion period of a char particle as seen in char combustion model. The density and the size of the pulverized coal in the mill duct system could also be reduced by some chemical demineralisation processes and this could provide more homogenous flow inside the mill duct system. For example, the studies on high volatile coal sizes below 62 and 500 μm showed that sulfur content was decreased from 2.4% and 2.6% to 1.3% to 1.4% while the ash content was decreased from 5% and 7.9% to 0.2% and 0.6% (Steel and Patrick, 2001, 2003). Therefore, total particle surface area disturbance in the duct system was analysed for base case duct, ND-01 and ND-02 duct systems as shown in Figure 11.

As a result, a ratio of the total particle surface area from each duct output compared to the total particle surface in the overall duct system was analysed for base case and alternative designs (ND-01 and ND-02). Maximum deviation value of total particle surface area in duct output from average particle surface area was %5.8, %2.8, and %5.1, for the base case, ND-01 and ND-02 models, respectively. Therefore, ND-01 design had better performance than ND-02 in the point of

homogeneity based on the particle disturbance in the duct system.

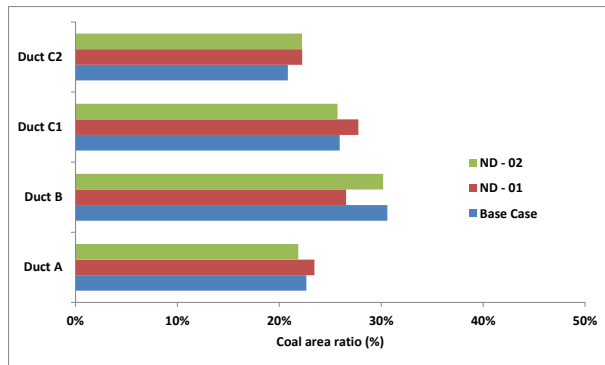


Figure 11. Coal distribution between duct outlets for 410 μm and bigger particle sizes

CONCLUSION

The mill duct system of the PCF Soma B Thermal PP was numerically analyzed by considering the measurements and performance tests performed in the PP. Performance tests showed that the boiler efficiency was deteriorated by 7.7%. This degradation was mainly due to the unburned carbon observed in the size larger than 500 μm in the boiler bottom ash. Feeding 51.8% of the coarse coal particles larger than 500 μm from the lowest level duct (Duct A) was also the reason for high amount of loss of ignition as they did not complete their combustion and fall down to the boiler bottom due to the insufficient residence time in the furnace area. More homogenous distribution of coal over 500 μm to the all level ducts were offered to solve this problem. The measured gas velocities, the rate of mass flow and coal size distribution to the ducts were generally consistent with the CFD results and provided assumptions. It was observed that the coal mass flow distribution was nearly uniform for the upper level ducts (Duct C1 and C2) of the mill duct system based on the validated base case CFD model results and PP tests; however, it was not uniform for the lower level ducts (Duct A and B). In order to resolve these problems in the mill duct system, two new alternative mill duct systems (ND-01 and ND-02) were designed with validated CFD analyses. Design comparisons showed that the coarse coal particles over 500 μm were more homogeneously dispersed in the new designed mill duct systems involved in Duct A. CFD results show that the maximum particle mass fraction deviation of total duct system from the average mass fraction of the total duct system for 410 μm and larger particles was obtained to be %12.2, %0.5, and %12.5 for, respectively, the base case duct system, ND-01 design, and ND-02 design. Furthermore, the maximum deviation value of total surface area of 410 μm and larger particles in duct system output from average surface area of 410 μm and larger particles is %5.8, %2.8, and %5.1, respectively, for base case duct system, for ND-01 design and for ND-02 design. Design comparisons have shown that the coarse coal particles larger than 230 μm are more homogeneously dispersed in the ND-01 design mill duct system involved in Duct A.

ACKNOWLEDGMENTS

The authors are very grateful to Soma Electricity Generation Cooperation for their technical assistance and support in developing experimental facilities and performing the experiments.

REFERENCES

- Ataş S., Tekir U., Paksoy M.A., Çelik A., Çam M. ve Sevgel T, Numerical and experimental analysis of pulverized coal mill classifier performance in the Soma B Power Plant, *Fuel Processing Technology*, 2014, 126, 441-452.
- Baum M.M., Street P.J., *Combustion science and technology*, 1971, 3(5), 231-24.
- Blondeau J., Kock R., Mertens J., Eley A.J., Holub L., Online monitoring of coal particle size and flow distribution in coal-fired power plants: Dynamic effects of a varying mill classifier speed, *Applied Thermal Engineering*, 2016, 98, 449-454.
- Chen J., Mann A. P., Kent J. H., Computational modelling of pulverised fuel burnout in tangentially fired furnaces, *Twenty-Fourth Symposium (International) on Combustion/ The Combustion Institute*, 1992/pp., 1381-1389
- Dodds, D., Naser, J., Staples, J., Black, C., Marshall, L., Nightingale, V., Experimental and numerical study of the pulverized-fuel distribution in the mill-duct system of the Loy Yang B lignite fuelled power station, *Powder Technology*, 207 (2011) 257-269.
- Ferrin J.L., Saavedra L., Distribution of the coal flow in the mill-duct system of the As Pontes Power Plant using CFD modelling, *Fuel Processing Technology*, 106 (2013) 84-94.
- Huber N., Sommerfeld M., Characterization of the cross-sectional particle concentration distribution in pneumatic conveying systems, *Powder Technology*, 79, 1994, 191-210.
- Kitto J.B., Stultz S.C., Steam: Its Generation and Use, ed. 41 *The Babcock & Wilcox Company*, 2005.
- Kozic M., Ristic S., Puharic M., Katavic B., Prvulovic M., Comparison of Numerical and Experimental Results for Multiphase Flow in Duct System of Thermal Power Plant, *Scientific Technical Review*, 2010, 60, 3-4, 39-47.
- Kuan B., Yang W., Schwarz M.P., Dilute gas-solid two-phase flows in a curved 90° duct bend: CFD simulation with experimental validation, *Chemical Engineering Science*, 62 (2007) 2068-2088.

Kuan B., Yang W., Solnordal C., CFD simulation and experimental validation of dilute particulate turbulent flows in a 90° duct bend, *Third International Conference on CFD in the Minerals and Process Industries*, Melbourne, Australia, 2003.

Parham J. J., Easson W. J., Flow visualisation and velocity measurements in a vertical spindle coal mill static classifier, *Fuel*, 2003; 82. 2115-2123.

Quick Reference Guide, *Storm Technologies*, Florida, USA, 2004.

Shah K.V., Vuthaluru R., Vuthaluru H.B., CFD based investigations into optimization of coal pulveriser performance: Effect of classifier vane settings, *Fuel Processing Technology*, 90 (2009) 1135-1141.

Singer J.G., Combustion fossil power, *Combustion Engineering INC*, Connecticut 1991

Steel K. M., Patrick J. W., The production of ultra clean coal by chemical demineralisation, *Fuel*, 2001, 80, 2019-2023

Steel K. M., Patrick J. W., The production of ultra clean coal by sequential leaching with HF followed by HNO₃, *Fuel*, 2003, 82, 1917-1920

Vijiapurapu, S., Cui, J., Munukutla, S., CFD application for coal/air balancing in power plants, *Applied Mathematical Modelling*, 30 (2006) 854-866.

Wydrych J., Borsuk G. ve Dobrowolski B., A numerical analysis of the flow through the elbow in the boiler pulverized coal system, *20th International Conference Engineering Mechanics*, Svatka, 2014.

Yang, W., Kuan, B., Experimental investigation of dilute turbulent particulate flow inside curved 90° bend, *Chemical Engineering Science*, 61 (2006) 3593-3601.



Ali Bahadır OLCAY received his B.S., M.S., and Ph.D. degrees in Mechanical Engineering from Middle East Technical University, Southern Illinois University Edwardsville and Southern Methodist University, respectively. He has worked as an adjunct professor at Southern Methodist University after his graduation. He joined the faculty of engineering at the University of Wisconsin in 2007. He also worked as a FEA / CFD consultant for Shaw Energy & Chemicals until his return to Turkey in 2010. He is currently a faculty member in the Department of Mechanical Engineering at Yeditepe University and his teaching and research interests are on thermal – fluid sciences.



Murat KAHRAMAN received his BSc in Mechanical Engineering Department from Yıldız Technical University in 2003 and received his MSc from Yıldız Technical University in 2006. He currently continues his PhD at Yeditepe University. He has been working as a senior researcher in Energy Institute of TUBITAK Marmara Research Center since 2007. His research interests are thermal power plant technologies, district heating systems and geothermal energy applications.



Selçuk ATAŞ is mechanical engineer and received his PhD degree from Istanbul Technical University in 2012. Also, he has been working as a researcher at TUBITAK Marmara Research Center Energy Institute since 2007. He has worked on many projects regarding power plant waste heat utilization, district heating design and optimization, heat accumulation systems, thermal power plant technologies, boiler baseline tests and tuning, performance monitoring of power plant components.